



A comprehensive techno-economic analysis for optimally placed wind farms

Sittichoke Pookpunt¹ · Weerakorn Ongsakul¹ · Nimal Madhu¹

Received: 17 July 2019 / Accepted: 5 May 2020
© Springer-Verlag GmbH Germany, part of Springer Nature 2020

Abstract

Wind power project development investment is based on the separate technical and financial analyses. Based on the actual wind data, data-based wind distribution map and wake effect model, a combined techno-economic analysis is proposed in this paper. Starting from deriving the wind distribution map, a comprehensive analysis extending to the feasibility assessment of the project is presented here. The problem is formulated as the maximization of net present value of the project subject to the specified initial investment cost within a fixed area and turbine spacing constraints. Simultaneous optimization of the wind turbine size, hub height and placement is realized with BPSO-TVAC. Sensitivity analysis and Monte Carlo simulation are used to investigate the feasibility of the project, against various parameters, imposed on by the techno-economic constraints. Hypothesis testing with a confidence level of 99.99% corroborates the results obtained from Monte Carlo simulation. With scenario analysis, a positive NPV is identified even in the worst-case scenario, an attractive trait for investors. An ideal decision-making tool considering technical efficiency and profitability simultaneously is presented.

Keywords Wind turbines placement · Wake effect model · Particle swarm optimization · Technical and financial analyses · Monte Carlo Simulation · Hypothesis Testing

1 Introduction

Wind turbines generating electrical energy from wind are grouped/operated together as a wind farm in order to increase the power production with merits including lower costs of installation, operation and maintenance. As a conventional wind farm layout, wind turbines are placed in rows that are 8–12 rotor diameters apart in the windward direction and in columns of 3–5 rotor diameters apart in the crosswind direction as the rule of thumb [1]. However, the different wind characteristic at specific areas may increase the wind farm array loss due to the wake effect reducing wind speed at a downstream turbine. An optimal wind farm layout, designed with a particular wind data, could reduce the wake effects and maximize both the total wind energy extraction and financial benefits to wind farm developers compared to the conventional wind farm layout [2].

Many layout optimization algorithms are available that can help to achieve the most efficient wind farm configuration that optimizes the placement of wind turbines, within a specific area, yielding higher power outputs with a denser and staggered layout. The optimal wind turbine placement is formulated as a combinatorial problem, using both analytical and heuristic optimization techniques, which determine the near-optimal wind turbine positioning in a wind farm. The location corresponding to the maximum energy production at the minimum cost is determined using the said formulation. Most studies apply heuristic search-based optimization algorithms including the genetic algorithm (GA) [3–7], evolutionary algorithm (EA) [6] and binary particle swarm optimization with time-varying acceleration coefficients (BPSO-TVAC) [8], but with the simplified wind data and turbine cost model.

Nonlinear mathematical programming approach utilizing the exact gradient information is developed to solve the continuous-variable wind farm layout optimization problem handling land-use constraints in [9]. Sequential convex programming (SCP) is employed to maximize the wind farm power production with a fixed large number of wind turbines in [10]. Both the heuristic methods in [3–8], as well

✉ Weerakorn Ongsakul
ongsakul@ait.ac.th

¹ Department of Energy, Environment and Climate Change,
School of Environment, Resources and Development,
Asian Institute of Technology, Pathumthani, Thailand

as the mathematical programming method in [9,10], have used only the simplified models for linear wake model, cost and wind distribution models. Layout optimization to reduce leveled cost of electricity generated from offshore wind farms is presented in [11]. Effect of different hub heights and uncertainty of wind is studied using linearization in [12,13]. Optimal layout for offshore wind farm considering wake effect and electrical losses is considered in [14]. The technical and financial analyses incorporating the actual wind data, investment cost on wind farm and uncertainty factors have not been considered in the previous literature.

To evaluate the feasibility of a wind farm planning project, both annual energy production and financial benefit should be considered. The historical wind data at specific sites are mostly used to represent the potential of energy production in the preliminary site investigation [15,16]. The variations in the speed and direction of wind are collected over a period of time and are transformed into the Weibull distribution function. A wind turbine power curve and the wind energy at a particular site can be evaluated using both the analytical and the numerical methods. In the wind farm evaluation, the array losses due to the wake effect need to be accounted for a wind farm considering the frequency associated with the range of speed and directional distribution of wind. Therefore, the variation of potential energy production from the observed wind speed at a specific site is estimated in [17–19]. Besides the wind farm energy production, an economic benefit evaluation is also considered as the wind farm design objective, which included cost of investment and cost of energy. In [2], an improved wake model based on the measured data [20] and the wind farm cost model using the combination cost model with the learning curve [21] is discussed. Using the actual wind speed and directional data, the wind distribution function is created and is then studied alongside the financial objective function. Maximizing the net present value (NPV), subject to both technical and economic constraints, which will directly maximize the shareholders' wealth, should be the evaluation criteria in the development of a wind farm.

For economic evaluation, wind farm project developer and many researchers usually follow the National Renewable Energy Laboratory (NREL) guideline manual [22]. The method provides the comparative analysis with the general economic indices including NPV, internal rate of return (IRR), profitability index (PI) or benefit-to-cost ratios, payback period (PB) and the cost of energy (COE). Generally, NPV is considered as the explicit and robust project evaluation method, derived from the discounted cash flows (DCF). In [23], EA is used to maximize the NPV, optimizing the wind farm configuration by using the simple cost model by fixing turbine cost ratio within a wind farm and simple wind distribution with the specific initial investment cost constraint. Moreover, the small number of the same wind turbine siz-

ing is used within the specific area of the wind farm. For the investment considerations, various technical inputs including the actual wind data, wind farm cost model and the different wind turbine sizing parameters are not used in the optimization. In addition to these, the financial inputs including the uncertainty of incomes, expense, and discount rates should be considered for accurate results.

Both technical and financial uncertainties impose investment risk on the NPV of a wind farm project. Sensitivity analysis and Monte Carlo simulation are used to consider the project risk to assure the investment returns both on energy production [24] and on financial evaluation [25,26]. Scenario analysis is developed to estimate the expected NPV to the specific variations in the key factors during an unfavorable event or to examine a theoretical worst-case scenario. Alternatively, the Monte Carlo simulations can provide the distributed project NPV as an outcome by repeating the calculation with the normally distributed input random variables. In [27], the variation in input parameter distribution including mean wind speed, Weibull shape factor, direction frequencies and power curve determined the AEP and NPV normal distributions for an existing wind farm. However, the study has not been applied to the development of a wind farm, especially considering the fact that the variation of NPV can be a useful tool for wind farm developers to make investment decision.

Generally, commercially available software is used to estimate the potential of energy production and to calculate the NPV using a given wind farm layout, which is also based on the experience of wind farm designer. The software does not optimize wind turbine placement and hence may not provide the highest possible NPV. In a previous study [2], on maximizing the annual operating income from a wind farm, making use of actual wind data and the wind farm cost model, a higher annual operating income is obtained compared to the conventional layout. However, the maximization of the annual operating income may not be similar to the maximum net present value for the entire wind farm project.

To summarize, the simultaneous techno-economic analysis incorporating the actual wind data, investment cost on wind farm and uncertainty factors is not considered previously. Maximizing NPV, subject to techno-economic constraints, is to be considered for maximization of stakeholder wealth in the development of a wind farm. For the investment considerations, the actual wind speed data, wind farm cost model and multiple wind turbine sizes and sizing parameters are not used. In terms of financial inputs, the uncertainty of incomes, expense and discount rates should be considered for accurate results. All the above-mentioned shortcomings are remedied in this paper.

In this research, using the wind turbine power curve along with the linear wake effect model, the power extraction and

annual energy from wind farm are determined. The initial wind farm investment cost is derived based on the wind turbine component cost model with a learning curve concept. The revenue and cash flow for a wind farm project lifetime are estimated. In a previous study conducted by the authors [28], to identify the optimal configuration of the wind turbines in the farm, binary particle swarm optimization (BPSO) is identified to be a suitable algorithm and hence the same approach is used in this study also. Here, the algorithm is employed to simultaneously determine the best configuration, sizing and hub height of wind turbines, which, in turn, maximizes the NPV subject for a fixed initial investment cost and fixed wind farm area constraints (both technical and financial). Sensitivity analysis and Monte Carlo simulation are used to determine the range and the normal distribution of NPV, respectively, assessing the variability of the NPV with respect to the wind resource. Hypothesis testing is also used to determine the feasibility of the project, and scenario analysis is implemented to determine the NPV in various scenarios including the worst. Hence, this study could be used as a comprehensive guide by an investor to design and assess the feasibility of a particular wind power project.

2 Wind farm model

2.1 Wind farm energy evaluation

Wind farms constitute turbine units, arranged in a particular fashion, aimed to increase the power generation. The energy production from the farm can be derived as the cumulative power production from each of the individual turbines in the farm. When the upstream turbine extracts power from the free-stream wind, it causes the turbulence and wind velocity deficit in the downstream turbine due to the wake effect. The array loss is accounted for by the wake loss lowering the total wind farm energy production.

2.1.1 Wake effect model

The single linear wake effect model used to determine the downstream wind speed was developed with full-scale experimental comparison in [29]. Because of the simplicity and the popularity due to its availability in commercial software, it is practical to embed this model in the population-based wind farm layout optimization process. Also, the combined techno-economic analysis being the point of focus, the choice of an even complex wake effect model, is not given prominence. Figure 1 presents the wake effect schematic as the boundary of linear expansion. Therefore, the wind speed of downstream turbine j affected by a wake from the upstream turbine i can be expressed as the wind speed deficit in (1), where u_{ij} is the wind speed in the wake, u_0 is the free-stream

wind speed, r_i is the upstream rotor radius and x_{ij} is the distance between upstream and downstream turbine.

$$\left(1 - \frac{u_{ij}}{u_0}\right) = \left(1 - \sqrt{1 - C_T}\right) \left(\frac{r_i}{(r_i + 2\alpha_1 x_{ij})}\right)^2 \tag{1}$$

The entrainment constant is the rate of wake expansion defined as $\alpha_1 = 0.5 \ln\left(\frac{z_0}{H}\right)$ where H is the hub height and z_0 is the surface roughness of a turbine location [30]. The thrust coefficient (C_T) is the fraction of the thrust or the axial force applied on a wind turbine rotor to the force of wind directly faced on the rotor plane which can be expressed by the axial induction factor (a) through the Betz relations as $C_T = 4a(1 - a)$ [1]. In addition, the different turbine hub heights deal with the wind speed varied by the different altitudes. The wind profile power law is used as a comparatively simple description with the reference height (H_{ref}) as in (2), where \bar{u}_H is the wind speed at altitude H , \bar{u}_{ref} is the wind speed at reference altitude H_{ref} and $\alpha_2 = \ln\left(\frac{z_0}{H}\right)$ is the altitude entrainment coefficient [30].

$$\bar{u}_H = \bar{u}_{ref} \left(\frac{H}{H_{ref}}\right)^{\alpha_2} \tag{2}$$

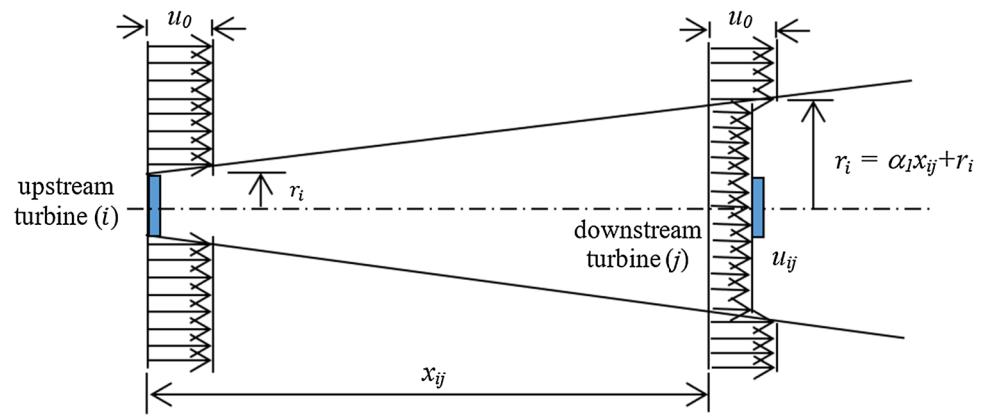
The combination of wake from multiple turbines is defined as the sum of individual loss of kinetic energy expressed as the square of the wind speed. Therefore, the total wind speed deficit at a downstream turbine (\bar{u}_j) from multiple wakes is determined by the sum squares of the individual deficits as in (3) [2], where N is the total number of wind turbines.

$$\left(1 - \frac{\bar{u}_j}{u_0}\right)^2 = \sum_{i=1, i \neq j}^N \left(1 - \frac{u_{ij}}{u_0}\right)^2 \tag{3}$$

2.1.2 Wind turbine power curve

The wind turbine power curve is the characteristic relating the electrical power generation from the turbine to the wind speed at a specific hub height. In general, turbine blades start rotating and delivery electrical power when the wind speed is higher than the cut-in speed (c_i). With the increase in wind speed, the turbine power output also increases with cubic proportionality, until it reaches the rated speed (c_r). The rated turbine power (T_R) is constantly generated as the wind speed increases from rated to cutout (c_o) value, where the blades are safely locked to prevent turbine failure. The turbine power curve model could be developed by a given cut-in, rated and cutout speeds as in (4). In this paper, turbine sizing index (T) from 1 to 8 represents 225 to 3000 kW turbine rating with different given hub heights (multiplier for standard hub height, $H = 1.0$). Specifications of Vestas series (V29 - V112) wind turbine rated power and one model of Shanghai

Fig. 1 Schematic representation of wake effect model



Electric Wind Power (W1250) are used here as shown in Table 1.

$$P_i(\bar{u}_i) = \begin{cases} 0 & : \bar{u}_i < c_i \\ \left(\frac{c_r - \bar{u}_i}{c_r - c_i}\right) T_R & : c_i \leq \bar{u}_i < c_r \\ T_R & : c_r \leq \bar{u}_i \leq c_o \\ 0 & : \bar{u}_i > c_o \end{cases} \quad (4)$$

The extracted electrical power from the wind turbine depends on the direction, intensity and probability of occurrence of the wind. Therefore, an average power generation from the wind farm (P_T) is obtained from the summation of power production from individual turbines and frequency of wind distribution in the direction around a wind farm as in (5), where f_k is the probability distribution of the calculated wind speed at direction k and N is the total number of turbines in the wind farm. Accordingly, the wind farm annual energy production (AEP) is determined as in (6):

$$P_T = \sum_{k=0}^{360} \sum_{i=1}^N f_k P_i(\bar{u}_i) \quad (5)$$

$$AEP = P_T * 8760. \quad (6)$$

2.2 Wind farm cost model

US Department of Energy and National Renewable Energy Laboratory (DOE and NREL) developed a reliable spreadsheet-based wind turbine cost model using the series empirical functions that relate the component mass and cost of the major components and subsystems [31]. The initial investment cost for the wind energy development is determined from the turbine sizing specification on the capital cost and the station cost (or balance of station cost). The turbine capital cost includes components like rotor, drive train and nacelle, tower, control, safety and monitoring systems. The station cost refers to the infrastructure implementation including foundation, transportation, road and civil, assembly and

installation, electrical interface and connection, engineering and permit.

In this paper, a wind farm cost model is developed by the learning curve to describe the lower of investment cost relating to a series production of a larger number of wind turbines installed within a wind farm. Purchasing a large number of similar turbines and using the common contribution infrastructure within a specific area will produce lower total project investment cost. The requirement of initial cost for the wind farm will be determined by the summation of the exponential learning curve following the technology factors (t_F) of the capital cost of the first turbine (TCC) and the balance of station cost (BOS) as in (7) [2], where IC_N is the total initial investment cost of turbines amount N units, t_{F1} and t_{F2} are the technology factor for turbine manufacturer and infrastructure implementation, respectively. The wind farm project is the basis of comparisons with similar product of the air craft industrial corresponding to the technology factor as between 0.90 and 0.95.

$$IC_N = \sum_{i=1}^N (TCC * i^{\ln(t_{F1})} + BOS * i^{\ln(t_{F2})}). \quad (7)$$

3 Wind farm project development

In general, the initial capital cost is the most important barrier affecting the competitiveness, hence the viability of the wind energy power generation. In Thailand, as the case study, a policy mechanism designed to accelerate investment in renewable energy (RE) technologies offers a long-term contract to every RE producers. In December 2014, National Energy Policy Council (NEPC) approved a feed-in tariff (FIT) at a fixed price of 6.06 Baht/kWh (19.5 cent/kWh) for a contract period of 20 years for wind energy generation [32] with 20% corporate income tax. Therefore, to develop a wind farm project, not only the wind energy potential in a specific

Table 1 Specifications of wind turbine series [31]

| Size index (T) | Model | Rated power (T_R) (kW) | Rotor diameter d_R , (m) | Standard hub height H (m) | Cut-in speed c_i m/s | Rated speed c_r m/s | Cut-out speed c_o m/s |
|--------------------|-------|----------------------------|----------------------------|-----------------------------|------------------------|-----------------------|-------------------------|
| 1 | V29 | 225 | 29 | 30 | 3 | 13 | 20 |
| 2 | V47 | 660 | 47 | 50 | 3.5 | 14 | 25 |
| 3 | V60 | 900 | 60 | 60 | 3.5 | 15 | 25 |
| 4 | W1250 | 1,250 | 70 | 70 | 3.5 | 15 | 25 |
| 5 | V82 | 1,650 | 82 | 80 | 3.5 | 15 | 25 |
| 6 | V90 | 2,000 | 90 | 90 | 3.5 | 15 | 25 |
| 7 | V100 | 2,600 | 100 | 100 | 3.5 | 15 | 25 |
| 8 | V112 | 3,000 | 110 | 115 | 3.5 | 15 | 25 |

location is to be evaluated, but it is also important to consider the cash flows while making a project investment decision.

3.1 Free cash flow

Free cash flow (CF) is the amount of money generated by a project after accounting for all capital expenditures. CF is used as the measure of a project’s financial performance and allows a project developer to pursue opportunities that enhance value of shareholders for the investor. It represents the amount of money that a company is able to generate after spending the money required to maintain or expand its asset base.

3.1.1 Initial outlay

Initial outlay (CF_0), given in (8), is the cost required to start the project including the initial cash flow and net working capital of investments such as project design and management, administration, new equipment and installation.

$$CF_0 = CF_{int} + NWC_0. \tag{8}$$

CF_{int} is the fixed capital investment and NWC_0 is the net working capital, at the initial stage. In this paper, CF_{int} including the capital cost of turbines and the base of station is determined by using NREL’s component cost model as shown in Table 1 and is assumed that NWC_0 is 5% of CF_{int} .

3.1.2 Annual after-tax operation cash flow (ATOCF)

$ATOCF$ over a project’s lifetime is the additional cash flow that a new project generates including energy sales as revenues, cost of operation, depreciation and taxation as given in (9). Rev_t is the revenues in the year t , NWC_t is the net working capital or the annual expense during the year t , and Dp_t is the depreciation in the year t .

$$ATOCF_t = ((Rev_t - NWC_t) * (1 - Tax_t)) + (Tax_t * Dp_t) \tag{9}$$

Here, revenues are the energy sale to the utilities, which is the product of AEP and feed-in-tariff (FIT). NWC_t is obtained from the annual operation and maintenance (O&M) using NREL’s component cost model. Dp is estimated using the modified accelerated cost recovery system (MACRS) used in the USA [33] and the straight-line methods for 10 years.

3.1.3 Terminal-year after-tax non-operating cash flow (TNOCF)

$TNOCF$ is the final cash flow, including both the inflows and outflows, at the end of the project’s life including a potential salvage value at the end of a machine’s life. $TNOCF$ can be calculated using (10), where T is the terminal year of project, Sal_T is the salvage value at terminal year T , BV_T is the book value of equipment at terminal year T , and NWC_T is the net working capital at the terminal year T .

$$TNOCF = Sal_T - ((Sal_T - BV_T) * Tax_T) + NWC_T. \tag{10}$$

In addition, the attractiveness of the project is evaluated based on the cash flows generated over the project lifetime. Using discounted cash flow analysis, the future cash flows over the project life are discounted back to the present value to determine net present value (NPV), internal rate of return (IRR) and profitability index (PI).

3.2 Discount rate

Discount rate (d) is the required rate of return used to discount a stream of future cash flows to their present value. It also accounts for the risk or uncertainty of future cash flows; the greater the uncertainty of future cash flows, the higher the

discount rate. To determine the appropriate discount rate, weighted average cost of capital (*WACC*), (11), is used if the project's risk profile is similar to that of the company. But if the project's risk profile is substantially different from that of the company, the capital asset pricing model (*CAPM*), (12), is used.

$$WACC : d = w_d \cdot r_d \cdot (1 - Tax) + w_e \cdot r_e \quad (11)$$

$$CAPM : d = r_f + \beta \cdot (r_m - R_f). \quad (12)$$

Here, w_d is the weight of debt value to the firm's financing, w_e is the weight of equity value to the firm's financing, r_d is the cost of debt, r_e is the cost of equity, r_f is the risk-free rate, β is the price movement index against market and $(r_m - R_f)$ is the equity market risk premium. The discount value is taken to be ranging between 8 and 12% during the optimization process and it will be accounting for an uncertainty with normal distribution during Monte Carlo simulation.

3.3 Net present value

Net present value (*NPV*) is a measure of profitability used in the capital budgeting to evaluate a project's potential return on investment. It is used to determine the present value of investment by discounted sum of all received cash flows which can be determined from the difference between the present values of cash inflow and outflow as in (13), where $ATOCF_t$ is the annual after-tax operation cash flow during the period t , $TNOCF$ is the terminal-year after-tax non-operating cash flow, CF_0 is the total initial outlay and d is the discount rate.

$$NPV = \sum_{t=1}^{T-1} \frac{ATOCF_t}{(1+d)^t} + \frac{ATOCF_T + TNOCF}{(1+d)^T} - CF_0. \quad (13)$$

3.4 Internal rate of return (IRR)

IRR is the interest rate or the discount rate (d) that makes a series of cash flows to a net present value of zero ($NPV = 0$) as in (14). IRR is used to compare with the minimum required rate of return on the investment to assess the feasibility with other projects.

$$0 = \sum_{t=1}^{T-1} \frac{ATOCF_t}{(1+IRR)^t} + \frac{ATOCF_T + TNOCF}{(1+IRR)^T} - CF_0. \quad (14)$$

3.5 Profitability index

Profitability index (*PI*) is the ratio between present value of the project's future cash flows and the initial investment used

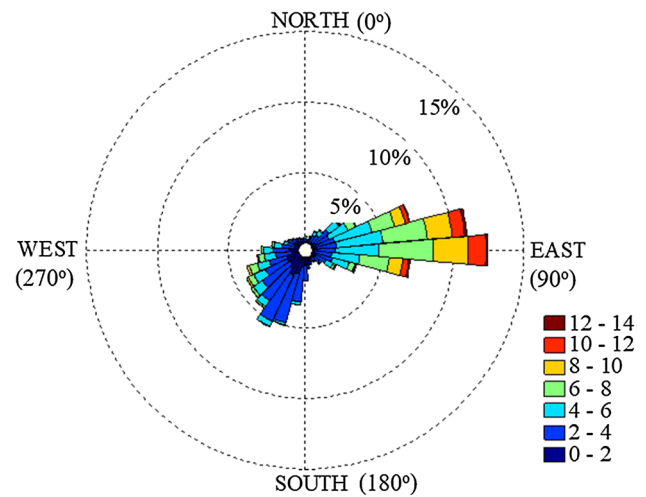


Fig. 2 Annual wind rose

to identify the relationship between the costs and benefits of a proposed project as shown in (15). The higher the value of *PI*, the more the financial attractiveness of the project, where the present value of the future cash flows is $\sum_{(t=1)}^{(T-1)} \frac{(ATOCF_t)}{(1+d)^t} + \frac{(ATOCF_T + TNOCF)}{(1+d)^T}$ and the initial investment cost is CF_0 .

$$PI = \frac{\text{(Present value of the future cash flows)}}{\text{(Initial investment cost)}} \quad (15)$$

3.6 Financial risk of wind farm project

Wind energy project is associated with a significant number of uncertain entities starting from the wind speed to required rate of return. Many financial analysis models attempt to predict the possibility of the outcomes of the project, relative to the intervention of the random input variables. Firstly, sensitivity analysis is used to determine the dependency of different variables and their impact, under a given set of assumptions. Here, the sensitivity of a specific number of input variables, including average wind speed, required rate of return, tax rate and expected salvage value, on the *NPV* of the project is investigated. Scenario analysis is used to estimate the expected dependent value responding to the specific changes in the key factor values of the unfavorable event, or to examine a theoretical worst-case scenario. Three scenarios, including pessimistic, most likely and optimistic, are used to determine the attraction of the wind farm project investment. Finally, Monte Carlo simulation is used to provide the estimation of the wind farm project *NPV* as an outcome by repeating the calculation with the random of AEP and discount rates according to the normal probability distribution.

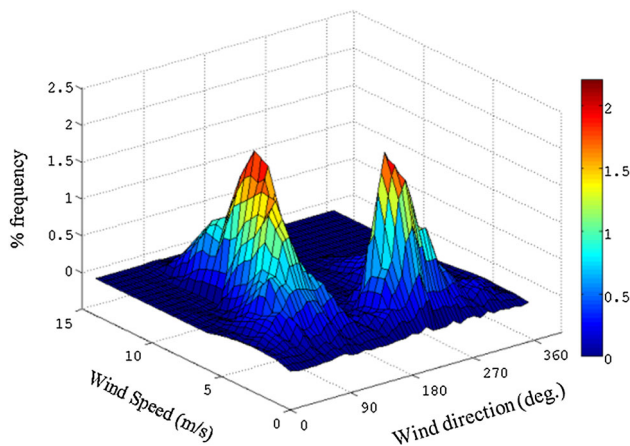


Fig. 3 Wind probability distribution map

4 Wind distribution map

Wind speed available at a particular height is the most important information required for a wind energy site. To determine potential of the site, wind data are transformed into a Weibull probability distribution function (WPDF) with scale (c) and shape (k) parameters [34]. Combining the WPDF with a turbine power curve, the annual wind energy production can be obtained. However, only the frequency of wind speed data is not sufficient for the potential evaluation of a wind farm site since the variation in the direction of wind will change the Weibull distribution characteristics leading to a variation in the energy production potential of the site [19]. Usually, the wind energy developer will consider a wind rose as the graphical tool describing the frequency of the wind speed and direction of flow, over a period of time at a specific location as shown in Fig. 2. (Graphical representation of wind speed at 40 meters is influenced by tropical northeast monsoon during November to April and southwest monsoon during May to October.) The frequency of free wind speed at any direction is divided into different color-level strips which represent the frequency of wind speed blowing from a particular direction. The longest strip shows the greatest frequency of wind speed over a specified time frame from that particular direction specified by the four cardinal directions corresponding to the degrees of a compass given as 0° or 360° for North (N), 90° for East (E), 180° South (S) and 270° for West (W).

Hourly wind speed and direction at 40 meters height is collected over a period of one year at Huasai District wind station, Nakhon Si Thammarat Province in Southern Thailand (latitude $8^\circ 4.376'$ N longitude, $100^\circ 27.513'$ E) [35]. The wind distribution map was developed as in [2] by integrating wind speed and direction into a wind frequency contour map as shown in Table 2. Wind frequency depends on the independent variables, the speed and direction of wind, as illustrated in Fig. 3. These wind data collected from Huasai

District have an average wind speed of 4.42 m/s at 40 meters height. The wind comes from two main directions due to the monsoon influence which blows from east during November to April and from southwest during May to October. If the wind data for a longer period are available, rolling multi-year average can be used to generate an annual wind distribution map. In general, a longer time-series data will be able to provide more reliability in a wind farm design. However, since the purpose is to develop the simultaneous financial and technical feasibility analysis of an optimal wind farm project, the data currently considered are only for a period of one year. Also, apart from the need for an averaging procedure, availability of a longer wind data shall not affect the methodology and the formulation is open-ended to accept the bigger data too.

Three average wind speed distribution maps are generated for 5 m/s, 5.5 m/s and 6 m/s, at 40 meters height with the same direction distribution as the Huasai site data. These higher average wind speeds with the same pattern are used as wind data input to determine the business opportunity comparison of wind farm with the different wind site potential.

5 Optimal placement of wind turbines

5.1 Problem formulation

To evaluate the NPV of the project, a wind farm business analysis model is illustrated in Fig. 4. With the required rate of return, NPV is obtained from the discounted project free cash flow as in (13), while IRR is obtained from discount rate with zero NPV and PI from (15). FCF is formed by FC_0 , $ATOCF$ and $TNOCF$ shown in (8)–(10), respectively. FC_0 is the initial investment cost of wind farm project to which a 5% add-up is made as the initial net working capital. $ATOCF$ is determined from the net profit and yearly depreciation, while $TNOCF$ is the terminal year of project including salvage and book value of project. In addition, a 5% add-up is also added to $TNOCF$ as the terminated net working capital. Project revenue is derived from the product of AEP and FIT, while yearly net working capital is the annual cash expense including the operation and maintenance cost (O&M) and the land lease cost (LLC), which is estimated to be 0.7% and 0.108% of AEP, respectively. The levelized replacement cost (LRC) is estimated to be 10.7 times of wind farm capacity as in [32].

Depreciation is accounted for 10 years of expense, and AEP is determined from the annual average power (PT) of wind farm as in (6). The different power generation in each turbine depends on its sizing as in Table 1 and its power curve as in (4) which is a function of turbine sizing ($T_{ij} \in 1, 2, \dots, 8$) and wind speed which is proportional to hub height multiplier ($H_{ij} \in 0.8, 0.9, \dots, 1.5$). The wake effect model in (1)

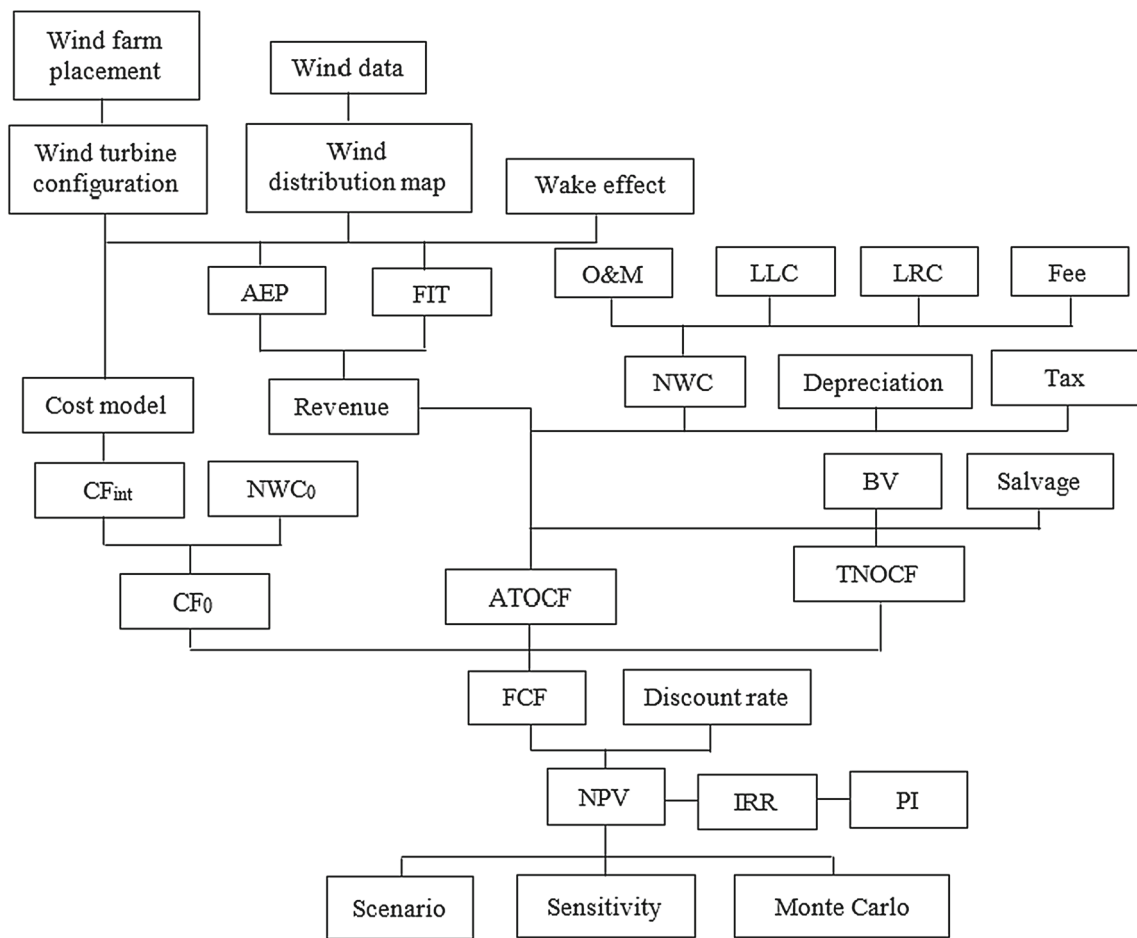


Fig. 4 Net present value evaluation of wind farm project

Table 2 Specifications of wind turbine series [31]

| u_0 (m/s) | Probability distribution of wind (% f_k) | | | | | | | | | | | |
|-------------|---------------------------------------------|--------|--------|--------|---------|---------|---------|---------|---------|---------|---------|---------|
| | 0–30 | 31–60 | 61–90 | 91–120 | 121–150 | 151–180 | 181–210 | 211–240 | 241–270 | 271–300 | 301–330 | 331–360 |
| 0 | 0.0126 | 0.0251 | 0.1006 | 0.0251 | 0.0251 | 0.1006 | 0.1635 | 0.1257 | 0.1257 | 0.1132 | 0.1132 | 0.0754 |
| 1 | 0.2138 | 0.2389 | 0.4401 | 0.2641 | 0.3269 | 0.7419 | 1.4083 | 1.0562 | 0.8424 | 0.5155 | 0.4275 | 0.2515 |
| 2 | 0.3395 | 0.6161 | 0.9808 | 0.9053 | 0.5030 | 1.0688 | 4.0111 | 3.5584 | 1.7352 | 0.8047 | 0.6035 | 0.2389 |
| 3 | 0.4778 | 1.4460 | 1.7855 | 1.5340 | 0.4024 | 0.8047 | 6.0606 | 3.9608 | 1.9992 | 0.9053 | 0.3772 | 0.3395 |
| 4 | 0.3395 | 1.8609 | 3.1560 | 1.8609 | 0.3898 | 0.2641 | 1.7855 | 1.7981 | 1.3328 | 0.8550 | 0.1132 | 0.1635 |
| 5 | 0.2263 | 1.4711 | 4.4386 | 1.8609 | 0.1257 | 0.0377 | 0.3395 | 0.9430 | 1.1568 | 0.4401 | 0.0377 | 0.0880 |
| 6 | 0.1383 | 0.9682 | 4.6398 | 1.7729 | 0.0754 | 0.0251 | 0.0629 | 0.7419 | 1.0059 | 0.1886 | 0.0251 | 0.0503 |
| 7 | 0.0629 | 0.4904 | 4.4386 | 1.3957 | 0 | 0.0126 | 0.0377 | 0.4401 | 0.6790 | 0.1006 | 0 | 0 |
| 8 | 0.0377 | 0.0629 | 3.6716 | 1.0939 | 0 | 0 | 0.0377 | 0.2012 | 0.3143 | 0.0503 | 0 | 0 |
| 9 | 0.0126 | 0.0629 | 2.3890 | 0.6790 | 0 | 0 | 0.0126 | 0.1006 | 0.1383 | 0.0126 | 0 | 0 |
| 10 | 0.0126 | 0.0126 | 2.0118 | 0.3018 | 0 | 0 | 0 | 0 | 0.0503 | 0 | 0 | 0 |
| 11 | 0.0126 | 0.0126 | 1.4460 | 0.2892 | 0 | 0 | 0 | 0 | 0 | 0 | 0 | 0 |
| 12 | 0 | 0.0126 | 0.7922 | 0.2138 | 0 | 0 | 0 | 0 | 0 | 0 | 0 | 0 |
| 13 | 0 | 0.0126 | 0.2389 | 0.0880 | 0 | 0 | 0 | 0 | 0 | 0 | 0 | 0 |
| 14 | 0 | 0.0126 | 0.0629 | 0.0126 | 0 | 0 | 0 | 0 | 0 | 0 | 0 | 0 |

is a function of distance between upstream and downstream turbine depending on wind farm placement ($S_{ij} \in 0,1$).

The linear wake model is used to determine the wind farm array losses because the result can be validated by most of the commercial software [32]. Mostly, wind farm layout optimization research prefers the linear model due to its simplicity and cost-effectiveness for the population-based algorithm. Moreover, the experiment shows the reasonable linear wake model compared to the other nonlinear wake models with the observed downstream wind speed at the actual wind farm site [18]. For this reason, the linear wake model as in (1) is used with the assumptions including (i) the frequency of wind speed and direction following the wind distribution map hit the first array of wind turbines as shown in Table 2, (ii) the wake effect linearly expands within a wind farm array without any disturbance from other circumstances, (iii) the turbines extract power with the constant coefficient of thrust ($CT = 0.88$) and (iv) the surface roughness length within a wind farm area is a constant value ($z_0 = 0.3$) as a plain topology of coastal environment.

Usually, a larger turbine size and higher hub height, which require a larger initial investment cost, can generate more power than a smaller turbine at a lower hub height. In this study, the initial investment cost increases from 20 M\$ to 200 M\$, which is used as the cost constraint on investment, and NPV was determined from a number of wind turbines with a specific sizing and hub height within a wind farm. Therefore, the problem formulation is given as follows:

$$\begin{aligned} &\text{Maximize fitness function}(S, T, H) \\ &= \sum_{t=1}^{T-1} \frac{ATOCF_t}{(1+d)^t} + \frac{ATOCT_T + TNOCF}{(1+d)^T} - CF_0, \end{aligned} \tag{16}$$

subject to

1. Number of wind turbines

$$0 < N_T = \sum_{i=1}^r \sum_{j=1}^c S_{ij} \leq r * c \tag{17}$$

2. Investment cost constraint

$$FC_{int}(S, T, H) \leq \text{Cost Constraint}, \quad \$ \tag{18}$$

where the cost constraint varies from 20 M\$ to 200 M\$

3. Revenue

$$Rev_t = AEP * FIT \quad \$/\text{year} \tag{19}$$

4. Annual energy production

$$\begin{aligned} AEP(S, T, H) &= \sum_{k=0}^{360} \sum_{i=1}^r \sum_{j=1}^c f_k \cdot S_{ij} \cdot P(T_{ij}, H_{ij}) \\ &*8760 \quad \text{kWh/year} \end{aligned} \tag{20}$$

5. Net working capital

$$\begin{aligned} NWC_t &= O\&M + LLC + LRCN \\ &+ Fee \quad \$/\text{year}, \end{aligned} \tag{21}$$

where

Operation and maintenance cost,

$$O\&M = 0.007 * AEP(S_{ij}, T_{ij}, H_{ij}) \quad \$/\text{year} \tag{22}$$

Land lease cost,

$$LLC = 0.00108 * AEP(S_{ij}, T_{ij}, H_{ij}) \quad \$/\text{year} \tag{23}$$

Levelized replacement cost,

$$LRC_N = 10.7 \sum_{i=1, j=1}^{r*c} P_R(T_{ij}) \quad \$/\text{year} \tag{24}$$

where r, c = number of cell rows (r=10) and columns (c=10).

Dp_t = Depreciation account for the straight line method of 10% CF_{int} for 10 years and another for MARSC method.

Sal_T = Salvage value at the end of project with 10% to 30% add-up.

NWC_0, NWC_T —Net working capital for initial and terminal years (5% of FC_{int}).

5.2 BPSO-TVAC for optimal wind farm placement

In this paper, the binary particle swarm optimization with time-varying acceleration coefficients (BPSO-TVAC) is used to optimally and simultaneously place the turbine positions, sizing and hub height in order to maximizing NPV of wind farm. BPSO-TVAC efficiently determines the optimal location for turbine placement in a wind farm layout optimization problem discussed in [8,28], while compared with other prominent algorithms. This information was ascertained when the particular formulation in this paper was tested with various optimization methods like genetic and evolutive algorithms, different versions of BPSO including features like time-varying, and random inertia weights and acceleration coefficients. In BPSO-TVAC, one particle representing a wind farm configuration is initialized randomly within a given particle population. If the number of particles is not well diversified, premature convergence can occur before reaching the near global optimum. A fixed wind farm

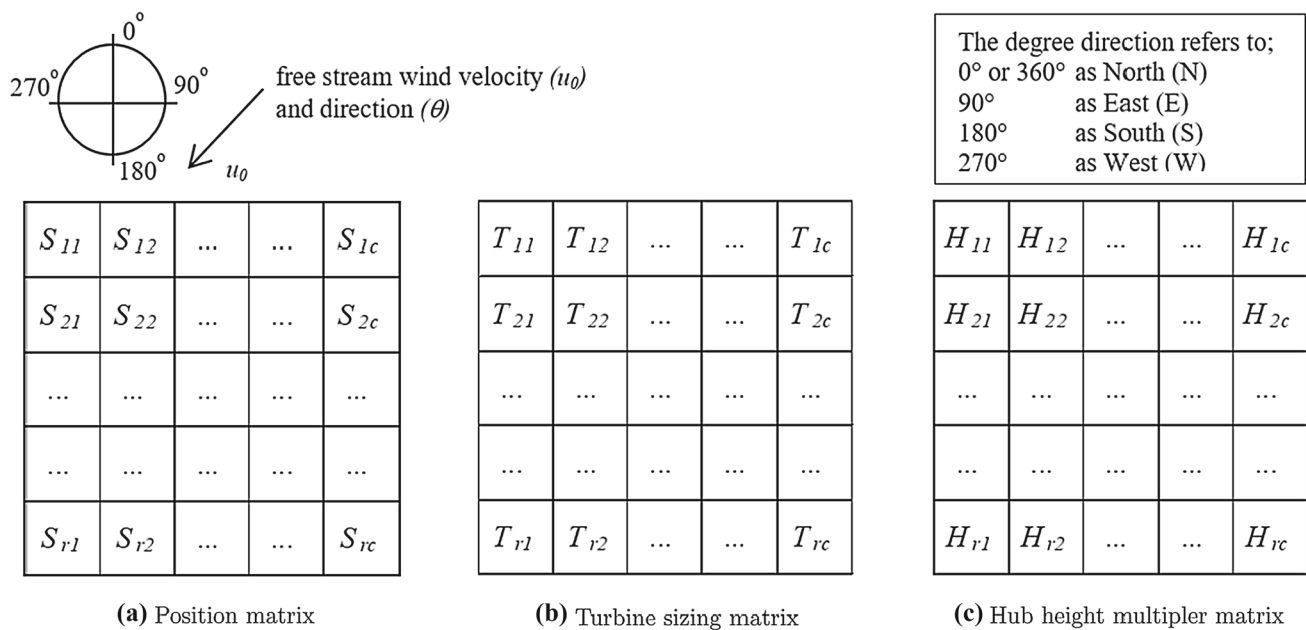


Fig. 5 Divided wind farm matrix representation in BPSO (particle)

area in the form of $10 \times 10 = 100$ cells in a matrix is considered. Three parameters in the configuration matrix will be optimally searched including 2-cell placement (0 or 1), 8 turbine sizing index ($T_{ij} = \{1, 2, \dots, 8\}$) and 8 turbine hub heights multiplier ($H_{ij} = \{0.8, 0.9, \dots, 1.5\}$). For 10×10 cells, the possible number of wind farm configurations is $8 \times 8 \times 2100$. To diversify the search, 50 population representing 50 possible wind farm configurations is optimized for their optimal control parameter within a reasonable computational effort. The procedure of BPSO-TVAC for optimal wind farm placement is described in [8].

A wind farm area of $2000 \times 2000 \text{ m}^2$ is divided into 10×10 square cell matrix, leaving a single cell with $200 \times 200 \text{ m}^2$ area or 200 meters spacing between adjacent turbines position. Initially, a wind farm as a particle is configured by three optimized parameters. The cell position thus randomly generated can have configurations as either exist (1) or not exist (0) in a wind farm position matrix, x_i^S , as shown in Fig. 5a. Subsequently, the sizing matrix of each wind turbine in a wind farm, x_i^T , is obtained as the element-wise product of matrices in Fig. 5a, b as in (25). The hub height multiplier matrix, x_i^H , is obtained by the element-wise product of matrices in Fig. 5a, c, as in (25).

$$\begin{aligned}
 x_i^S &= \begin{bmatrix} S_{1,1} & S_{1,j} & \dots & S_{1,c} \\ \dots & & & \\ S_{r,1} & S_{r,j} & \dots & S_{r,c} \end{bmatrix} \quad | \quad i = 1 : r, j = 1 : c \\
 x_i^T &= [S_{i,j} \cdot T_{i,j}] \\
 x_i^H &= [S_{i,j} \cdot H_{i,j}]
 \end{aligned} \quad (25)$$

The overall procedure to evaluate the wind farm optimization is shown in Fig. 6. Firstly, the wind farm area characteristic definition includes area size, turbine spacing, roughness, restricted zone and area level. When a wind distribution map at specific average wind speed is generated, the wind farm configuration parameters including wind turbine placement, sizing and hub height will be optimized. By using BPSO-TVAC, the initial input parameters including particle positions and velocities are randomly generated. Here, 50 particles and 500 maximum iterations are used in this paper. The cost constraint is varied from 20 Mto200M and is defined in each initial iteration. During the optimization process, if the investment cost of the updated configuration particles from a previous iteration exceeds its initial cost constraint, the sizing will be randomly reduced until the given cost constraint is satisfied. If not possible, the number of turbines is randomly removed until the cost constraint is satisfied. The personal best positions (pbest) and the global best position (gbest) as the fitness function need to be evaluated. Consequently, an updated position for each particle is determined by the probability threshold of the sigmoid function which is a function of updated velocity.

6 Results and discussion

6.1 Wind farm optimal placement at the maximum NPV

BPSO-TVAC is used to simultaneously optimize wind turbines placement, sizing and hub height maximizing NPV

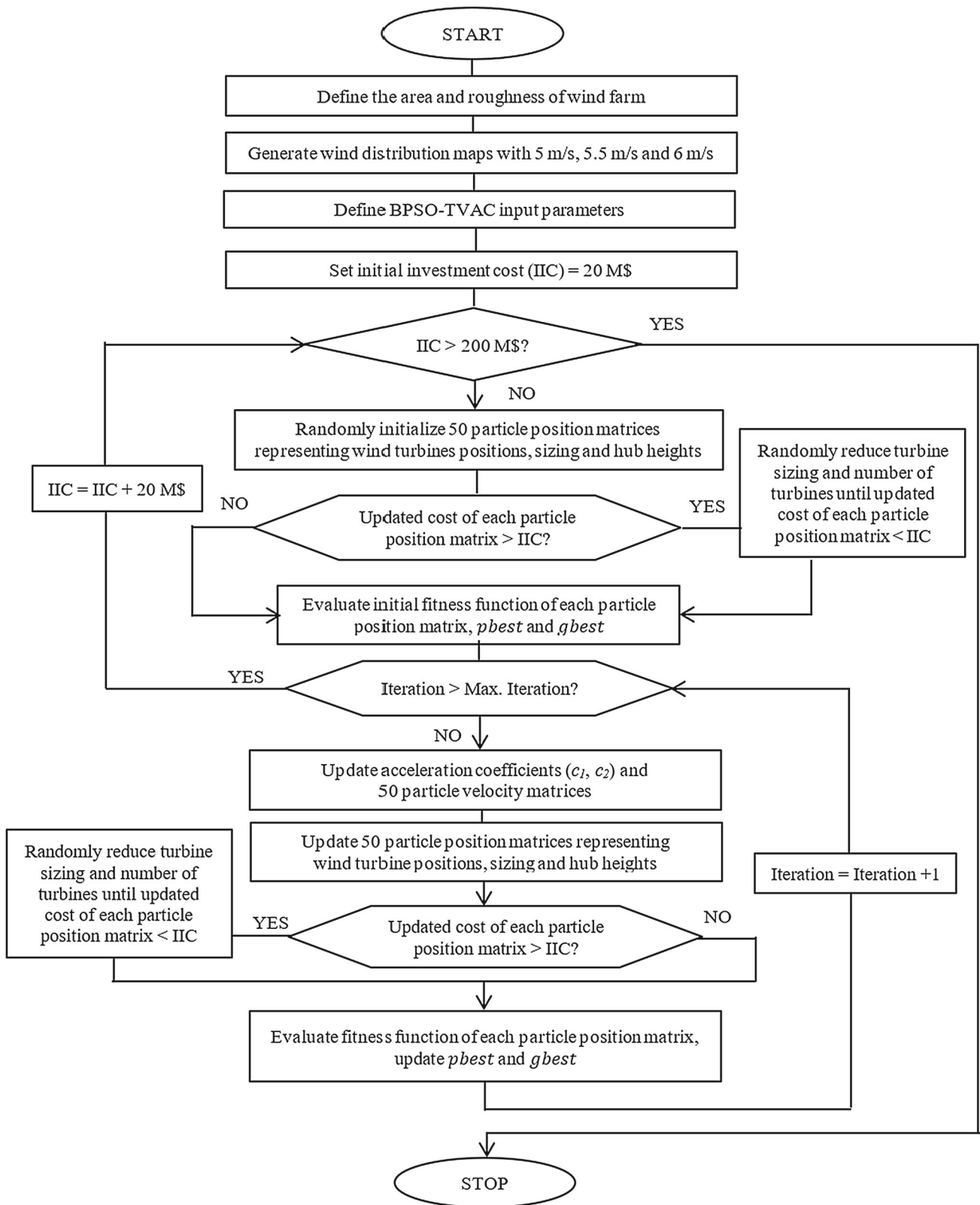
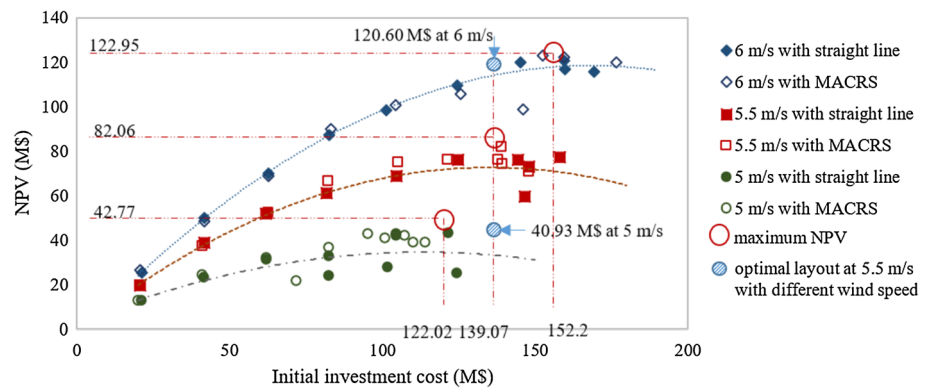
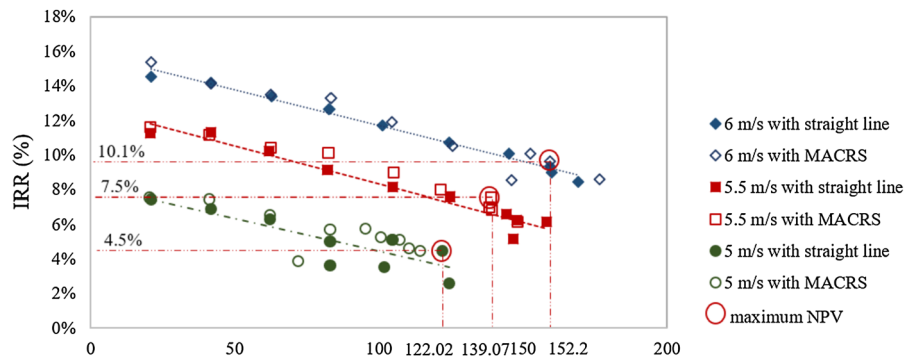


Fig. 6 Overall procedure of wind farm layout optimization

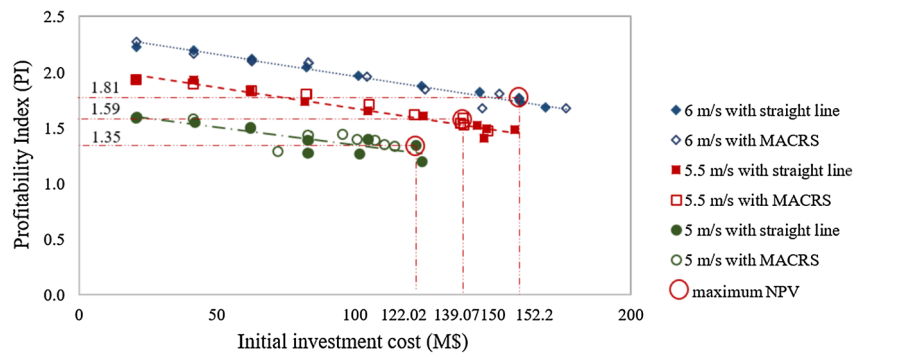
Fig. 7 Comparison of wind farm NPV, IRR, and PI with investment costs, for various average wind speed values and depreciation methods



(a) NPV vs. investment costs



(b) IRR vs. investment costs



(c) PI vs. investment costs

Table 3 Comparison of the maximum NPV between the different average wind speed of the optimal placement and depreciation methods with the same 10% discount rate

| Average wind speed | 5 m/s | | 5.5 m/s | | 6 m/s | |
|--------------------|--------|---------------|---------|---------------|---------|---------------|
| | MACRS | Straight line | MACRS | Straight line | MACRS | Straight line |
| NPV (M\$) | 42.30 | 42.77* | 82.06* | 77.39 | 122.95* | 121.03 |
| IRR | 5.8% | 4.5% | 7.5% | 6.1% | 10.1% | 9% |
| PI | 1.44 | 1.35 | 1.59 | 1.49 | 1.81 | 1.76 |
| Initial Cost (M\$) | 95.22 | 122.02 | 139.07 | 158.20 | 152.52 | 159.47 |
| Revenue (M\$/year) | 20.33 | 24.41 | 32.80 | 35.04 | 40.98 | 41.97 |
| AEP (GWh/year) | 104.28 | 125.17 | 168.21 | 179.70 | 210.17 | 215.27 |
| COE (cent/kWh) | 12.14 | 12.84 | 11.06 | 11.70 | 9.79 | 10.00 |
| Wake loss | 15.4% | 18.1% | 23.7% | 26.5% | 24.7% | 27.9% |

Fig. 8 Comparison of wind farm AEP between the average wind speed with the same distribution in the different initial investment cost and depreciation methods

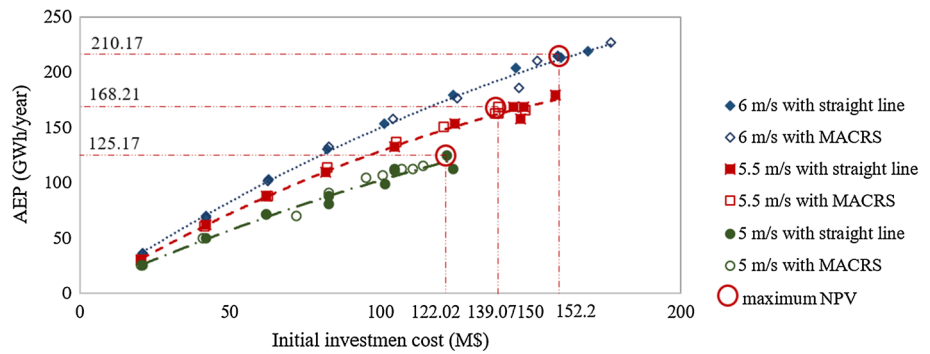
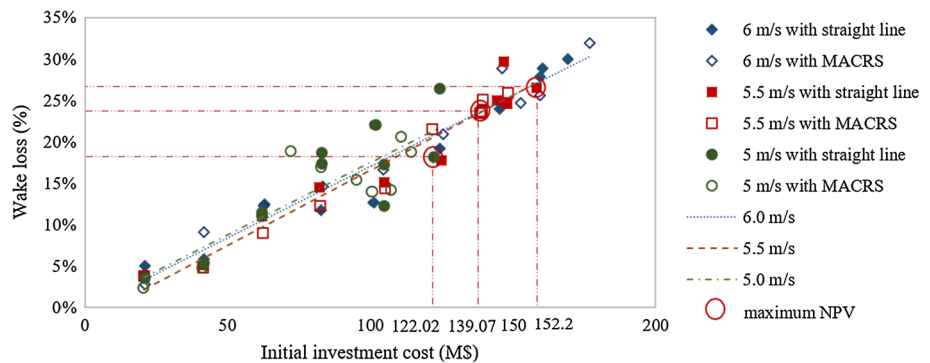


Fig. 9 Wind farm wake loss following the initial investment cost



using the wind distribution map at 5, 5.5 and 6 m/s average wind speed at 40 meters' height with the same 10% discount rate. With the same average wind speed, the NPV increases with the initial investment cost, but the IRR linearly declines. With the same investment cost, a higher average wind speed provides a larger maximum NPV and IRR than the equal initial investment costs as shown in Fig. 7a, b. At wind speed of 6.0 m/s, the higher investment is the increase in NPV until it reaches the maximum NPV of 122.95 M\$ at the optimal 152.52 M\$ of investment cost. If the investment cost is higher than 152.52 M\$, the NPV will decline because of the higher wake loss. The profitability index or benefit of cost ratio linearly declines as the investment cost is higher as shown in Fig. 7c. For the average wind speed at 6 m/s, 5.5 m/s and 5 m/s, they obtain the maximum NPV of 122.95 M\$, 82.06 M\$ and 42.77 M\$ with the initial investment cost at M\$152.52, 139.07 M\$ and 122.02 M\$, respectively. It corresponds to 10.1%, 7.5% and 4.5% of IRR as shown in Table 3. Moreover, the optimal placements show little difference between the 10 years of depreciation on both MACRS and straight-line method. When using the optimal configuration at a particular wind speed on other average wind speeds, their NPV will be lower than those of other optimal configurations. For instance, using the fixed 5.5 m/s optimal layout on the 5 m/s wind speed, the calculated NPV of 40.93 M\$ would be 50% lower than the maximum 5.5 m/s NPV of 82.06 M\$ and 4.5% lower than 5.0 m/s maximum NPV of 42.77 M\$. Meanwhile, using the fixed 5.5 m/s optimal layout on the 6 m/s wind speed, the calculated NPV of 120.60 M\$ would be

47% higher than the maximum 5.5 m/s NPV of 82.06 M\$ and 2% lower than 6.0 m/s maximum NPV of 122.95 M\$ as shown in Fig. 7a.

A higher investment cost provides a larger AEP as shown in Fig. 8. However, the maximum NPV will not correspond to the largest AEP because the slope of AEP declines as an investment cost is higher. In Fig. 9, it can be noticed that the wake loss in the optimal wind farm layouts linearly increases with a higher investment cost. For different average wind speeds, the linear wake loss increases with the investment cost showing the array loss of wind farm for a specific wind direction. At the maximum NPV for different wind speeds, a higher average wind speed provides the larger wake loss because more turbines are located within the wind farm.

Within a given square 2000*2000m² wind farm area, the configuration of wind turbine placements at their maximum NPV and the convergence of calculations with the average wind speed at 5 m/s, 5.5 m/s and 6 m/s are shown in Figs. 10, 11 and 12, respectively. BPSO-TVAC locates most of the largest sizing wind turbines at the edge of wind farm area directly facing the most frequent wind direction from north-east and southwest monsoon following the wind distribution map in Fig. 3. The algorithm also suggests increasing the hub height to capture higher wind speed compared to standard altitudes. Also, the turbines inside the area are sparsely installed to reduce the wake loss effect. Although the wake loss arises on using a larger number of turbines, within a higher average wind speed area, larger investment cost can

| | | | | | | | |
|-------|-------|-------|-------|--|-----|--|-------|
| T=8 | | | T=8 | | | | T=8 |
| H=1.5 | | | H=1.5 | | | | H=1.5 |
| T=8 | | | T=8 | | | | T=8 |
| H=1.5 | | | H=1 | | | | H=1.2 |
| | | T=8 | | | | | T=8 |
| | | H=1.5 | | | | | H=1.5 |
| | | T=8 | | | T=8 | | T=8 |
| | | H=1 | | | H=1 | | H=1 |
| | T=8 | | | | | | T=8 |
| | H=1.5 | | | | | | H=1.5 |
| | T=8 | | | | | | T=8 |
| | H=1.5 | | | | | | H=1 |
| | T=8 | | | | | | T=8 |
| | H=1.5 | | | | | | H=1.5 |
| T=8 | | T=8 | | | | | T=8 |
| H=1 | | H=1 | | | | | H=1.5 |
| T=8 | | | T=8 | | | | T=8 |
| H=1 | | | H=1 | | | | H=1.5 |
| T=8 | | | T=8 | | | | T=8 |
| H=1.5 | | | H=1.5 | | | | H=1.5 |

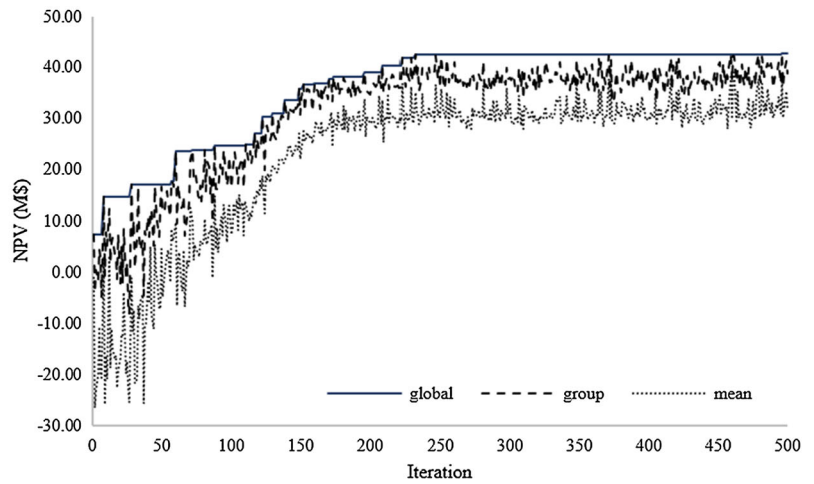


Fig. 10 Wind farm configuration for 5 m/s wind speed and convergence characteristics

| | | | | | | | | |
|-------|-------|-------|-------|--|-------|-------|--|-------|
| T=8 | | T=8 | | | T=8 | | | T=8 |
| H=1.5 | | H=1.5 | | | H=1.5 | | | H=1 |
| T=8 | | | | | T=8 | | | T=8 |
| H=1 | | | | | H=1 | | | H=1 |
| T=8 | | | T=8 | | | | | T=8 |
| H=1.2 | | | H=1 | | | | | H=1.5 |
| T=8 | | | T=8 | | | | | T=8 |
| H=1 | | | H=1.5 | | | | | H=1 |
| T=8 | | T=8 | | | | T=8 | | T=8 |
| H=1.5 | | H=1 | | | | H=1.5 | | H=1 |
| T=8 | | T=8 | | | T=8 | | | T=8 |
| H=1.5 | | H=1 | | | H=1 | | | H=1 |
| | | T=8 | | | | | | T=8 |
| | | H=1 | | | | | | H=1 |
| T=8 | | | | | T=8 | | | T=8 |
| H=1.5 | | | | | H=1 | | | H=1 |
| | T=8 | | | | | | | T=8 |
| | H=1.5 | | | | | | | H=1 |
| T=8 | | | T=8 | | T=8 | | | T=8 |
| H=1 | | | H=1 | | H=1 | | | H=1.5 |

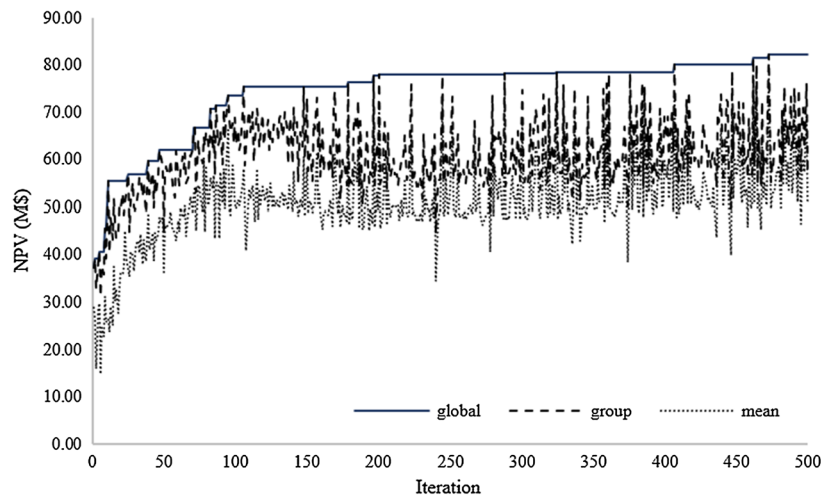


Fig. 11 Wind farm configuration for 5.5 m/s wind speed and convergence characteristics

| | | | | | | | | | |
|-------|--|-----|-------|-----|-------|-------|--|--|-------|
| T=8 | | | T=8 | | | T=8 | | | T=8 |
| H=1 | | | H=1.5 | | | H=1 | | | H=1.5 |
| T=8 | | | | T=8 | | | | | T=8 |
| H=1.5 | | | H=1.5 | | | | | | H=1.2 |
| T=8 | | | | | T=8 | | | | T=8 |
| H=1.2 | | | | | H=1.5 | | | | H=1.2 |
| T=8 | | | | | T=8 | | | | T=8 |
| H=1.5 | | | | | H=1.5 | | | | H=1 |
| | | | | | T=8 | | | | T=8 |
| | | | | | H=1 | | | | H=1 |
| | | | | | | T=8 | | | T=8 |
| | | | | | | H=1.5 | | | H=1 |
| | | | | | | | | | T=8 |
| | | | | | | H=1 | | | H=1.2 |
| T=8 | | T=8 | | | | | | | T=8 |
| H=1.5 | | | | | T=8 | | | | H=1 |
| T=8 | | T=8 | | | T=8 | | | | T=8 |
| H=1.5 | | H=1 | | | H=1.5 | | | | H=1 |
| | | T=8 | | | T=8 | | | | T=8 |
| | | H=1 | | | H=1.5 | | | | H=1 |
| T=8 | | | | | T=8 | | | | T=8 |
| H=1.5 | | T=8 | | | H=1 | | | | H=1.5 |

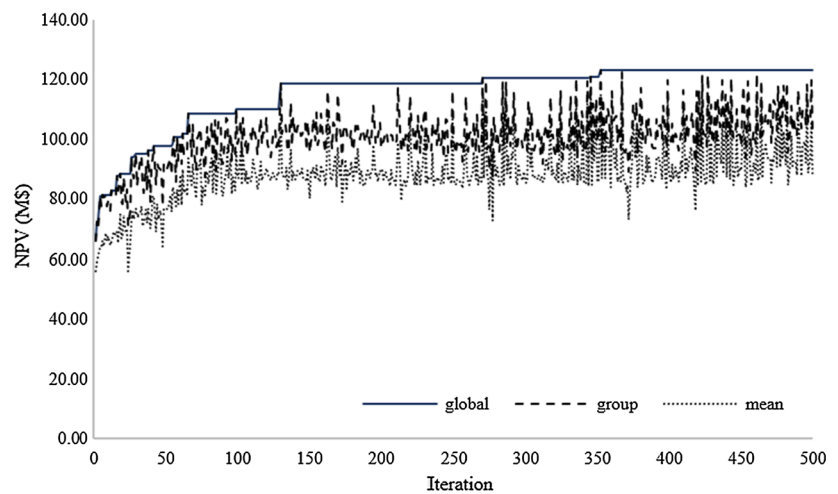
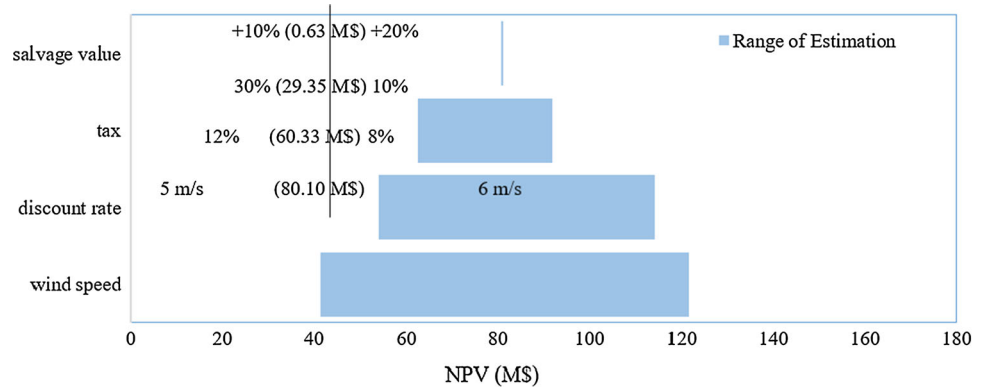


Fig. 12 Wind farm configuration for 6 m/s wind speed and convergence characteristics

Table 4 Sensitivity level and range of estimation at 5.5 m/s average wind speed

| Dependent variable | | | |
|----------------------------------|--------|--------------|---------------|
| AEP (GWh/year) | 168.21 | Project life | 20 years |
| Annual expense (M\$/year) | 3.05 | FIT (\$/kWh) | 0.195 |
| Initial investment cost (M\$) | 132.45 | Depreciation | Straight line |
| Investment working capital (M\$) | 6.62 | | |
| NPV of baseline (M\$) | 80.75 | | |
| Independent variable | | | |
| | Low | Base | High |
| Salvage value (M\$) | 10.60 | 11.66 | 12.72 |
| Tax rate | 10% | 20% | 30% |
| Discount rate | 12% | 10% | 8% |
| Average wind speed (m/s) | 5.0 | 5.5 | 6.0 |
| Sensitive variables | | | |
| NPV to salvage value (M\$) | 80.43 | 80.75 | 81.06 |
| NPV to tax rate (M\$) | 91.90 | 80.75 | 62.55 |
| NPV to discount rate (M\$) | 114.28 | 80.75 | 53.95 |
| NPV to wind speed (M\$) | 41.40 | 80.75 | 121.51 |

Fig. 13 Range of estimation for independent variable during sensitivity analysis



receive a higher NPV and IRR than those with lower average wind speed.

6.2 Sensitivity analysis

Sensitivity analysis is used to determine the variation in an dependent variable with a particular independent one, under a given set of assumptions. Here, the specific input variables including average wind speed, required rate of return, tax rate and expected salvage value are varied one at a time to assess the extent of impact on the NPV. The base average wind speed, discount rate, tax rate and salvage value are 5.5 m/s, 10%, 20% and 11.66 M\$, respectively. The low-to-high ranges of average wind speed, discount rate, tax rate and salvage value are 5.0–6.0 m/s, 12%–8%, 30%–10% and 10.60–12.57 M\$, respectively, as shown in Table 4. The project assumes a fixed FIT of 0.195 \$/kWh, 20 years lifetime and the 10% straight-line depreciation method for 10 years.

The range of estimation shows the sensitivity level of an independent variable to the project NPV. As shown in Fig. 13, the site average wind speed from 5 to 6 m/s is the most sensitive variable leading to the NPV ranging from 41.40 to 121.51 M\$, respectively. The discount rate varying from 12% to 8% is the second most sensitive variable leading to the NPV range from 53.95 to 114.28 M\$, while the tax rate ranging from 30% to 10% leads to the NPV range from 62.55 to 91.90 M\$. The expected salvage value has little impact to project NPV because of the highest 20 years discounted value.

6.3 Monte Carlo simulation analysis

The random variables influencing the analysis of the said project considered here are the wind speed and the required rate of return or the discount rate. Monte Carlo simulation can provide the estimation of the normally distributed NPV of the wind farm project, by using the normally distributed AEP and discount rates. Here, the probability of AEP depends on the

Fig. 14 Monte Carlo simulation histogram result

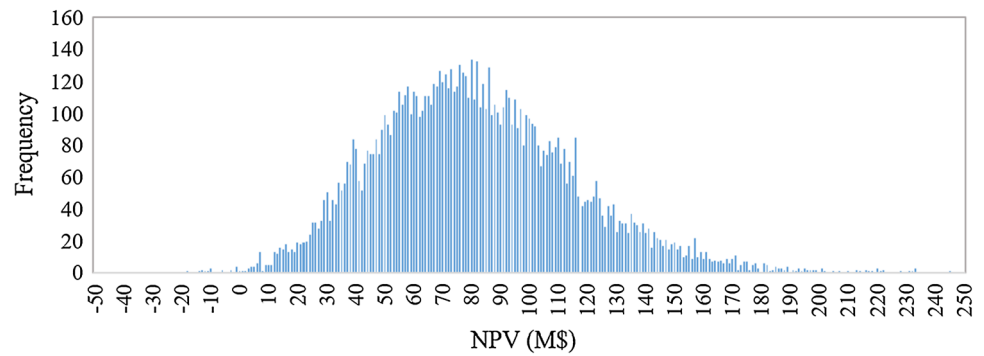
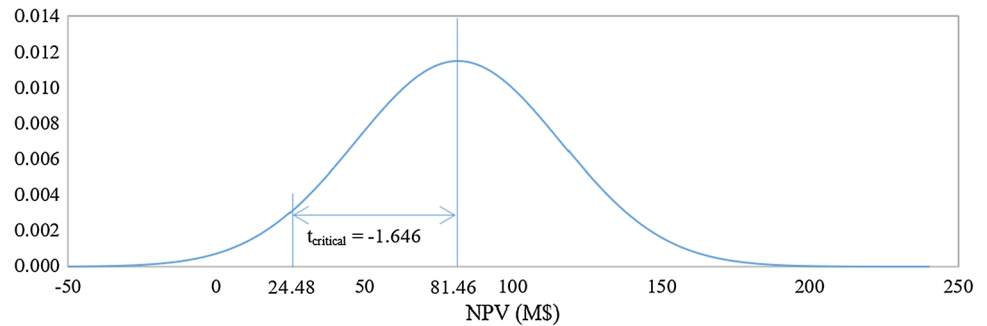


Fig. 15 Monte Carlo simulation result with normal distribution of project NPV



average wind speed in the range, 5.0–6.0 m/s, and the range of discount rate is between 8% and 12%. Sampling of NPV calculation from normal distribution of AEP and discount rate is shown in Table 5.

Figure 14 shows the frequencies of different outcomes generated by a 10,000 time of simulation generating the discrete project NPV which should be a normal distribution if the sampling size is large enough as in Fig. 15. The mean NPV is 81.46 M\$ at the middle of the curve implying a 50% that the actual return will be higher or lower than the mean. The 95% confidence level of NPV is more than 24.48 M\$ as shown in Table 6. The highest NPV and lowest NPV of simulation are 281.74 M\$ and -18.38 M\$, respectively. The base NPV from Table 4 is 0.87% different from the Monte Carlo simulation.

6.4 Hypothesis test

Hypothesis testing is the process to judge and evaluate whether a hypothesis is likely to be true or false, within a certain confidence level. Suppose the weight average cost of capital (WACC) is 6%, the expected IRR should be higher than 6% or NPV should be larger than 66.35 M\$. The null hypothesis is $NPV \leq 66.35$, while the alternate being $NPV > 66.35$. When the null hypothesis is rejected, the alternative one is accepted. To carry out hypothesis testing of NPV, one-tailed test should be used.

Therefore, the null and alternative hypothesis are:
 $H_0 : NPV_h \leq 66.35$ (Null) and $H_a : NPV_h > 66.35$ (Alternative)

Test statistic is calculated based on the number of NPV sampling carried out in Monte Carlo simulation within 5% significance level ($\alpha = 0.05$) using (26), where μ is the mean NPV of the project, σ is the standard deviation and n_s is the number of samplings from Monte Carlo simulation. The t test results are indicated in Table 7. Because t test statistics is -43.62 much smaller than -1.646 (-5% significance level) leading to rejecting H_0 hypothesis, we could infer that the NPV of this wind farm project is very likely to be higher than 66.35 M\$, that also with a confidence level of 99.99%.

$$t_{stat} = \frac{NPV_h - \mu}{\sigma / \sqrt{n_s - 1}} \quad (26)$$

6.5 Scenario analysis

Scenario analysis is used to estimate the expected dependent value responding to the specific changes in the values of key factors during unfavorable events or to examine a theoretical worst-case scenario. Here, three scenarios are used, namely pessimistic, most likely and optimistic. As shown in Table 8, pessimistic scenario uses 5 m/s average wind speed with 30% tax rate, 12% discount rate and 11% salvage value. Most likely scenario uses 5.5 m/s average wind speed with 20% tax rate, 10% discount rate and 12% additional salvage value. Optimistic scenario uses 6 m/s average wind speed with 10% tax rate, 8% discount rate and 13% salvage value. The result indicates that the pessimistic scenario still provides the positive NPV and IRR of 15.86 M\$ and 2.37%, respectively.

Table 5 Sampling of NPV calculation from the normal distribution in AEP and discount rate

| Fixed value variable | | Normal distribution variable | | | | |
|------------------------------------|----------------|------------------------------|------------------------|--------------------|-----------|----------|
| FIT (\$/kWh) | = 0.195 | Discount rate | | | | |
| Annual expense (\$/kWh) | = 0.018 | AEP | | | | |
| Initial investment (M\$) | = 132.45 | | | | | |
| Tax | = 20% | | | | | |
| NWC0 and NWCT (M\$) | = 6.62 | | | | | |
| Salvage value (M\$) | = 15.89 | | | | | |
| Year | AEP (GWh/year) | Revenue (M\$/year) | Annual exp. (M\$/year) | Depreciation (M\$) | CF (M\$) | PV (M\$) |
| 1 | 137.09 | 26.73 | 2.48 | 11.92 | 21.78 | 19.64 |
| 2 | 141.29 | 27.55 | 2.56 | 11.92 | 22.37 | 18.19 |
| 3 | 208.34 | 40.62 | 3.78 | 11.92 | 31.86 | 23.36 |
| 4 | 164.74 | 32.12 | 2.99 | 11.92 | 25.69 | 16.99 |
| 5 | 183.61 | 35.80 | 3.33 | 11.92 | 28.36 | 16.91 |
| 6 | 163.56 | 31.89 | 2.96 | 11.92 | 25.53 | 13.72 |
| 7 | 168.11 | 32.78 | 3.05 | 11.92 | 26.17 | 12.68 |
| 8 | 144.49 | 28.17 | 2.62 | 11.92 | 22.83 | 9.98 |
| 9 | 149.45 | 29.14 | 2.71 | 11.92 | 23.53 | 9.27 |
| 10 | 178.75 | 34.85 | 3.24 | 11.92 | 27.67 | 9.83 |
| 11 | 111.31 | 21.70 | 2.02 | 0 | 15.75 | 5.05 |
| 12 | 235.31 | 45.88 | 4.26 | 0 | 33.29 | 9.62 |
| 13 | 120.94 | 23.58 | 2.19 | 0 | 17.11 | 4.46 |
| 14 | 170.77 | 33.30 | 3.10 | 0 | 24.16 | 5.68 |
| 15 | 198.27 | 38.66 | 3.59 | 0 | 28.05 | 5.94 |
| 16 | 124.86 | 24.35 | 2.26 | 0 | 17.67 | 3.37 |
| 17 | 169.18 | 32.99 | 3.07 | 0 | 23.94 | 4.12 |
| 18 | 128.43 | 25.04 | 2.33 | 0 | 18.17 | 2.82 |
| 19 | 230.29 | 44.90 | 4.17 | 0 | 32.58 | 4.56 |
| 20 | 195.68 | 38.15 | 3.55 | 0 | 47.02 | 5.94 |
| Project evaluation sampling result | | | | | NPV (M\$) | 63.06 |
| | | | | | IRR | 5.80% |

Table 6 NPV range of the project using Monte Carlo simulation

| | | | |
|-------------------------------|--------|---------------------------|--------|
| Number of sampling | 10,000 | Max NPV (M\$) | 281.74 |
| Mean NPV (M\$) | 81.46 | Min NPV (M\$) | -18.38 |
| 95% of confidence level (M\$) | 24.48 | Standard deviation of NPV | 34.64 |

Table 7 NPV range of the project using Monte Carlo simulation

| | | | |
|-------------------------------|---------|---------------------------|--------|
| Mean NPV(\$ μ) | 81.46 | Degree of freedom | 99.99 |
| Variance | 1200.26 | $t_{critical}$ | -1.646 |
| Number of samplings (n_s) | 10,000 | t test statistics (tstat) | -43.62 |
| Hypothesized NPV_h | 66.35 | p value | 0 |

Table 8 Inferences from scenario analysis

| Variable | Pessimistic | Most likely | Optimistic |
|--------------------------------------------|-------------|-------------|------------|
| Average wind speed (m/s) | 5.0 | 5.5 | 6.0 |
| AEP (at max. NPV, GWh/year) | 104.28 | 168.21 | 210.17 |
| Annual expense (\$/kWh) | 0.0192 | 0.0181 | 0.0167 |
| Initial investment cost (M\$) | 90.69 | 132.45 | 145.26 |
| Investment in working capital (M\$) | 4.53 | 6.62 | 7.26 |
| Depreciation (10 years straight line, M\$) | 8.16 | 11.92 | 13.07 |
| Salvage value (M\$) | 6.35 | 11.66 | 15.69 |
| Tax rate | 30% | 20% | 10% |
| Discount rate | 12% | 10% | 8% |
| Result of scenario analysis | | | |
| NPV (M\$) | 15.58 | 80.75 | 192.21 |
| IRR | 2.34% | 7.23% | 13.45% |

7 Conclusion

In this paper, technical and financial analyses for a wind farm project development, considering the linear wake loss using the actual wind distribution map, are effectively carried out. The optimal wind turbine placement in the farm is set to maximize the net present value of wind farm subject to the given initial investment cost and fixed wind farm area constraints. Binary particle swarm optimization (BPSO) efficiently and simultaneously optimizes wind farm configuration including wind turbine placement, sizing and hub height. The obtained optimal initial investment cost could lead to the highest NPV, maximizing shareholders' wealth. Sensitivity analysis indicates that the site average wind speed and discount rate are the top most sensitive factors to the NPV. The Monte Carlo simulation dealing with the uncertainties of both normally distributed average wind speed and discount rate provides a normally distributed NPV. Hypothesis testing can ensure with 99.99% confidence level that the NPV would be more than 66.35 M\$. Finally, the scenario analysis provided positive NPV obtained for the worst-case scenario, which can be useful for wind farm developers to make investment decision for a particular wind farm project.

References

- Patel MR (2006) Wind and solar power system, 2nd edn. Taylor & Francis, New York, pp 81–82
- Pookpant S, Ongsakul W (2016) Design of optimal wind farm configuration using a binary particle swarm optimization at Huasai district, Southern Thailand. *Energy Convers Manag* 108:160–180
- Emami A, Noghreh P (2010) New approach on optimization in placement of wind turbines within wind farm by genetic algorithms. *Renew Energy* 35:1559–1564
- Khanali M, Ahmadzadegan S, Omid M, Nasab F, Keyhani, Chau KW (2018) Optimizing layout of wind farm turbines using genetic algorithms in Tehran province, Iran. *Int J Energy Environ Eng* 9(4):399–411
- Evangelopoulos VA, Georgilakis PS (2014) Optimal distributed generation placement under uncertainties based on point estimate method embedded genetic algorithm. *IET Gen Transm Distrib* 8(3):389–400
- Kirchner-Bossi N, Porté-Agel F (2018) Realistic wind farm layout optimization through genetic algorithms using a Gaussian wake model. *Energies* 11(12):1
- Chen Y, Li H, He B, Wang P, Jin K (2015) Multi-objective genetic algorithm based innovative wind farm layout optimization method. *Energy Convers Manag* 105:1318–1327
- Pookpant S, Ongsakul W (2013) Optimal placement of wind turbines within wind farm using binary particle swarm optimization with time-varying acceleration coefficients. *Renew Energy* 55:266–276
- Guirguis D, Romero DA, Amon CH (2016) Toward efficient optimization of wind farm layouts: utilizing exact gradient information. *Appl Energy* 179:110–123
- Park J, Law KH (2015) Layout optimization for maximizing wind farm power production using sequential convex programming. *Appl Energy* 151:320–334
- Pillai AC, Chick J, Khorasanchi M, Barbouchi S, Johanning L (2017) Application of an offshore wind farm layout optimization methodology at Middelgrunden wind farm. *Ocean Eng* 139:287–297
- MirHassani S, Yarahmadi A (2017) Wind farm layout optimization under uncertainty. *Renew Energy* 107:288–297
- Wang L, Cholette ME, Zhou Y, Yuan J, Tan AC, Gu Y (2018) Effectiveness of optimized control strategy and different hub height turbines on a real wind farm optimization. *Renew Energy* 126:819–829
- Amaral L, Castro R (2017) Offshore wind farm layout optimization regarding wake effects and electrical losses. *Eng Appl Artif Intell* 60:26–34
- Zeljko D, Milulovic J (2012) Assessment of the wind energy resource in the South Banat region, Serbia. *Renew Sustain Energy Rev* 16:3014–3023
- Shata A S Ahmed, Hanitsch R (2006) Evaluation of wind energy potential and electricity generation on the coast of Mediterranean Sea in Egypt. *Renew Energy* 31:1183–1202
- Serrano-Canalejo C, Sarrias-Mena R, García-Triviño P, Fernández-Ramírez LM (2019) Energy management system design and economic feasibility evaluation for a hybrid wind power/pumped hydroelectric power plant. *IEEE Lat Am Trans* 17(10):1686–1693

18. Gul M, Tai N, Huang W, Nadeem MH, Yu M (2019) Assessment of wind power potential and economic analysis at Hyderabad in Pakistan: Powering to local communities using wind power. *Sustain* 11(5):1
19. Chaurasiya PK, Kumar VK, Warudkar V, Ahmed S (2019) Evaluation of wind energy potential and estimation of wind turbine characteristics for two different sites. *Int J Ambient Energy* 1:1–11
20. Brogna R, Feng J, Sørensen JN, Shen WZ, Porté-Agel F (2020) A new wake model and comparison of eight algorithms for layout optimization of wind farms in complex terrain. *Appl Energy* 259:114189
21. Song D et al (2020) Optimal design of wind turbines on high-altitude sites based on improved Yin–Yang pair optimization. *Energy* 193:116794
22. SW, PDJ, HT (1995) A Manual for the Economic Evaluation of Energy Efficiency and Renewable Energy Technologies. NREL Tech Rep NREL/TP-462-5173
23. González JS, Rodríguez ÁGG, Mora JC, Payán M Burgos, Santos JR (2011) Overall design optimization of wind farms. *Renew Energy* 36:1973–1982
24. Mora EB, Spelling J, van der Weijde AH, Pavageau E-M (2019) The effects of mean wind speed uncertainty on project finance debt sizing for offshore wind farms. *Appl Energy* 252:113419
25. Shin H, Baldick R (2018) Mitigating market risk for wind power providers via financial risk exchange. *Energy Econ* 71:344–358
26. Judge F et al (2019) A lifecycle financial analysis model for offshore wind farms. *Renew Sustain Energy Rev* 103:370–383
27. Afanasyeva S, Saari J, Kalkofen M, Partanen J, Pyrhönen O (2016) Technical, economic and uncertainty modelling of a wind farm project. *Energy Convers Manag* 107:22–33
28. Pookpant S, Ongsakul W (2016) Design of optimal wind farm configuration using a binary particle swarm optimization at Huasai district, Southern Thailand. *Energy Convers Manag* 108:160–180
29. Jensen NO (1983) A Note on Wind Generator Interaction. Riso National Laboratory, Riso National Laboratory RISO-M-2411, Nov 1983
30. Sun H, Yang H (2020) Numerical investigation of the average wind speed of a single wind turbine and development of a novel three-dimensional multiple wind turbine wake model. *Renew Energy* 147:192–203
31. Pierrot M (2005) Wind turbines and wind farms database. http://www.thewindpower.net/manuturb_turbines_en.php
32. Ananjanich P (2015) Thailand: Renewable Energy Policy Update. In: Chrometzka T (ed) New Power Development Plan announced in May (Status May 2015). German Federal Ministry for Economic Affairs and Energy: German Federal Ministry for Economic Affairs and Energy, p 4
33. Service D. o. t. T. I. R. (2015) How To Depreciate Property. vol Publication 946, D. o. t. T. I. R. Service, Ed., ed. Department of the Treasury Internal Revenue Service: Department of the Treasury Internal Revenue Service, p 114
34. Saeed MA, Ahmed Z, Yang J, Zhang W (2020) An optimal approach of wind power assessment using Chebyshev metric for determining the Weibull distribution parameters. *Sustain Energy Technol Assessm* 37:100612
35. Eurek K, Sullivan P, Gleason M, Hettinger D, Heimiller D, Lopez A (2017) An improved global wind resource estimate for integrated assessment models. *Energy Econ* 64:552–567

Publisher's Note Springer Nature remains neutral with regard to jurisdictional claims in published maps and institutional affiliations.